

Sample-size dependence of the superconducting transition of ribbon-shaped Pb nanocrystals studied by scanning tunneling spectroscopy

Ze-Lei Guan,¹ Yan-Xiao Ning,¹ Can-Li Song,^{1,2} Jian Wang,³ Jin-Feng Jia,² Xi Chen,² Qi-Kun Xue,^{2,1} and Xucun Ma^{1,*}

¹*Institute of Physics, Chinese Academy of Sciences, Beijing 100190, China*

²*Department of Physics, Tsinghua University, Beijing 100084, China*

³*The Center for Nanoscale Science and Department of Physics, The Pennsylvania State University, University Park, Pennsylvania 16802, USA*

(Received 28 November 2009; revised manuscript received 21 January 2010; published 22 February 2010)

We have systematically investigated the superconductivity of single crystalline Pb nanoribbons grown on Si substrates by using low temperature scanning tunneling microscopy/spectroscopy. Superconductivity transition is observed in the nanoribbons with a width ~ 10 nm and a thickness of 2.9 nm. By studying the width dependence of the superconducting parameters T_c and H_{c2} , a dimensional crossover between two dimensions and one dimension is identified.

DOI: [10.1103/PhysRevB.81.054516](https://doi.org/10.1103/PhysRevB.81.054516)

PACS number(s): 74.78.Na, 74.62.Bf, 74.70.Ad, 75.75.-c

When the diameter of superconducting nanowires is comparable to or smaller than the superconducting coherence length, the superconductivity of the nanowires exhibits one-dimensional (1D) or quasi-one-dimensional behaviors. This has attracted much attention due to both fundamental interest and potential applications.¹⁻⁹ In this regime, Cooper pairs are squeezed into a very small volume, their wave functions are strongly modified; thus, the quantum confinement effect in transverse dimensions on the superconducting order parameter becomes important. The thermal and quantum fluctuations of the superconducting order parameters⁷ will play a dominating role and therefore suppress the superconductivity.² To address these issues, single crystalline nanowires with atomic level-controlled sizes¹⁰⁻¹³ are required. However, the nanowires studied so far usually suffer from some uncertainties, such as the presence of disorder and defects.^{10,11,13-18} Particularly, precise size control of an individual superconductive nanowire and its transport measurement still remain a great technical challenge.

Recently, we have developed a method by which highly ordered arrays of superlong Pb nanoribbons with atomic level-controlled thickness and width could be prepared on Si substrates by molecular beam epitaxy (MBE). The method employs a nanoscale template of the Al-decorated Si(111) surfaces, where the width and thickness of the Pb nanoribbons are precisely controlled by the Al (less than 1 ML) and Pb coverages, respectively.¹⁹ The superconductivity of such nanostructures can be studied *in situ* by a scanning tunneling microscope (STM) operated at low temperature and under magnetic field. The latest progress in this aspect includes the study of quantum size effects in two-dimensional (2D) thin films and nanoislands of Pb.²⁰⁻²⁶ Here, we report the atomic scale-dependent superconducting properties of the Pb nanoribbons by using STM/STS.

Our experiments were carried out in an ultrahigh vacuum (UHV) low temperature STM system combined with a MBE chamber (Unisoku USM-1300 and RHK SPM-1000). By simultaneously heating and pumping the low temperature insert, the STM samples can be maintained at a temperature range of 2.2–50 K by liquid ⁴He cooling. A magnetic field up to 7 T can be applied along the direction perpendicular to the

sample surface. After *in situ* preparation of nanoribbons on Si (111) substrate (As-doped, 1–5 m Ω cm) with a miscut of $\pm 0.3^\circ$ in the MBE chamber, as described in the previous study,¹⁹ the samples were transferred to the STM stage for STM/STS measurements. The tunneling conductance spectra (dI/dV) were acquired using the standard lock-in technique with a small ac modulation of 0.2 mV at a frequency of 2 kHz. The tunneling junction was set at $V_{\text{bias}}=10$ mV, $I=0.2$ nA. All STM/STS measurements were carried out by using PtIr tips.

Figure 1(a) shows the normalized dI/dV spectra of a nanoribbon at temperature from 2.60 to 6.85 K. The Pb nanoribbon is 3.72 nm (13 ML) thick and 36 nm wide. The superconducting gap is clearly visible at 2.60 K, and completely disappears at 6.85 K. The behavior is also seen in the zero bias conductance (ZBC) in Fig. 1(b). Using the tunneling spectra acquired near the transition temperature, we find that ZBC scales linearly to the temperature. By extrapolating the linear relationship of ZBC versus T at the point where ZBC=1, the superconductivity transition temperature, T_c , is calculated as 6.49 K. With the same fitting procedure, we obtain a T_c of 6.39 K for a narrower ribbon with a width of 15 nm, as shown in Figs. 1(c) and 1(d). Despite a more than doubling of the width, the two nanoribbons with the same thickness exhibit nearly the same T_c (the difference is only 0.1 K). The data for a series of nanoribbons are summarized in Table I. Although some data are missing (for example, 12 ML is unstable against quantum size effect¹⁹⁻²¹ and cannot be prepared), several interesting features can be observed in Table I.

First, a 2.86 nm (10 ML) thick and 10 nm wide crystalline Pb ribbon shows robust superconductivity. Second, the T_c decreases when either width or thickness decreases. As discussed above, the thickness has a more significant effect on the T_c than the width. A change in two times in the width leads to a change in approximately 0.1 K in T_c . However, the same T_c change is observed with only a 2% change in thickness. This is reminiscent of the “2D” nature of the nanoribbons regarding the large aspect ratio of width/thickness.

The suppression of T_c by reducing width may result from the 1D dissipations in Pb nanoribbons due to thermal and

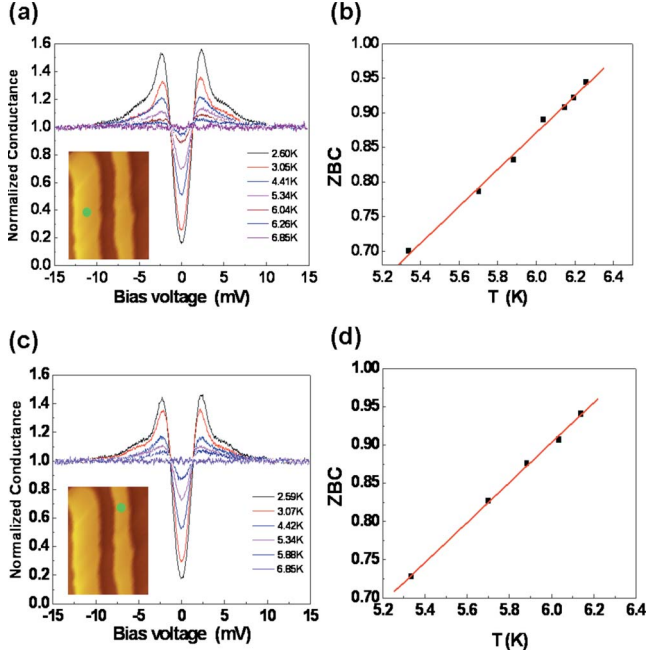


FIG. 1. (Color online) (a) and (c) A series of normalized tunneling conductance spectra of (a) 36 nm and (c) 15 nm wide Pb nanoribbons with a thickness of 13 ML (3.72 nm). The spectra were acquired by locating the tip at the green point in the insert STM image at different temperatures from 2.60 to 6.85 K. The scale of the STM image is $160 \times 200 \text{ nm}^2$. The left nanoribbon in the image is 36 nm wide, while the right 15 nm. (b) and (d) Temperature-dependent zero bias conductance (ZBC) for (b) 36 nm and (d) 15 nm wide nanoribbons.

quantum fluctuations,² which can induce phase slips and destroy the superconductivity in certain local regions of the ribbons below T_c . In addition, at reduced width, the increasing lateral quantum confinement on electron movement lowers the screening potential and promotes the effective Coulomb repulsion between electrons. The enhanced Coulomb interaction suppresses the superconductivity in very narrow ribbons.^{10–12} Compared to a nanoisland with the same thickness but a lateral size $>83 \text{ nm}$ (the coherence length of the bulk Pb), a difference of 0.46 K in T_c can be seen for the 36 nm wide ribbon and an island with a size of $\sim 300 \text{ nm}$. The difference is large and cannot be derived from the simple scaling up of the difference of T_c (0.1 K) between the 15 and 36 nm nanoribbons. The result indicates that from large island to 36 nm wide ribbon, the superconducting Pb crosses from a quasi-2D to a quasi-1D superconductor.

The magnetic property of nanoribbons is then studied systematically. The upper critical field shown in Table I was extracted from the magnetic field dependent tunneling spectra. Figure 2(a) shows a series tunneling spectra of a 3.15 nm (11 ML) \times 60 nm nanoribbon measured at magnetic fields from zero to 0.75 T at 3.32 K. The suppression of the superconducting gap and the increase in ZBC are visible with increasing magnetic field. The superconductivity is completely destroyed at $\sim 0.65 \text{ T}$. To accurately determine the critical magnetic field, we first analyze the evolution of the ZBC vs the applied magnetic field. For classical type II superconductors, when a field H ($H_{c_1} < H < H_{c_2}$) is applied, the

TABLE I. Critical temperatures (T_c) and upper critical magnetic fields (H_{c_2}) measured on Pb nanoribbons of different thicknesses and widths. The data of H_{c_2} were obtained at a fixed temperature ($T=4.32 \text{ K}$).

Thickness	Width (nm)	T_c (K)	H_{c_2} ($T=4.32 \text{ K}$)
2.9 nm (10 ML)	10	6.20	1.46
	23		1.16
	37	6.40	0.82
	51		0.44
	102		0.29
3.15 nm (11 ML)	16		1.38
	22	6.32	1.07
	23		1.01
	30		0.91
	42	6.41	0.64
	60		0.63
	>83 (island)	6.68	
3.72 nm (13 ML)	13		1.44
	15	6.39	1.37
	17		1.29
	31		0.81
	36	6.49	0.62
	50		0.54
>83 (island)	6.95		

magnetic field penetrates the superconductor in the form of vortex. The localized states in the vortex cores lead to a linear quasiparticle excitation at the Fermi level since the population of the vortices scales proportionally to the field. Therefore, a linear dependence of ZBC vs H is expected, as observed recently in Pb islands.²⁴ However, it is not the case here. We observed a linear dependence of the $(ZBC)^{1/2}$, not ZBC , with H above 0.18 T and a near plateau below 0.18 T, as shown in Fig. 2(b). The field dependence of $(ZBC)^{1/2}$ might result from the reduced mean-free length in this two-dimensional confined system, which will be discussed below. One possible origin is the suppression of the superconducting order parameters via incomplete Meissner effect in low dimensional superconductors, such as superconducting nanowires,¹⁴ which usually causes a stronger quasiparticle excitation at the Fermi level. By extrapolating the linear relationship of $(ZBC)^{1/2}$ vs H at the point where $ZBC=1$, we estimated the upper critical field H_{c_2} of the nanoribbons. The result is summarized in Table I.

The upper critical field also can be determined by the Ginzburg-Landau (GL) theory with Gor'kov's addition.²⁷ For a small ratio of the film thickness to the penetration depth λ , the field dependence of the energy gap Δ obeys an empirical equation $(\Delta/\Delta_0)^2 = 1 - (H/H_c)^2$, indicative of a second order phase transition near H_{c_2} . We obtained the field dependence of $\Delta(H)$ by analyzing the field-dependent tunneling spectra using Dynes function,^{22,28} in which the broaden-

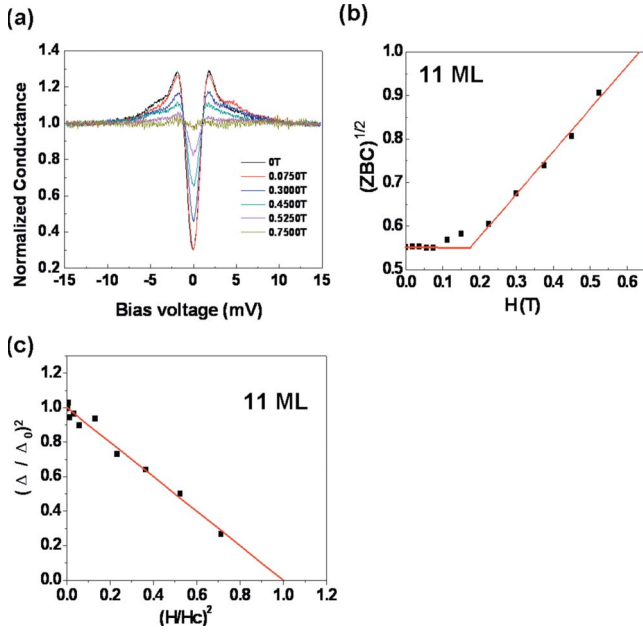


FIG. 2. (Color online) (a) Magnetic field-dependent normalized conductance spectra for an 11 ML thick and 60 nm wide Pb nanoribbon. (b) Magnetic field dependence of $(ZBC)^{1/2}$ measured from zero to 0.75 T. The lines are a guide for the eye. (c) Energy gap (Δ) of the ribbon vs magnetic field (H). The line is a fit based on Ginzburg-Landau-Gor'kov theory.

ing effect based on BCS theory was included. The range of broadening factor is 0.4 ± 0.2 meV at 3.32 K. We found that the dependence obeys the equation $(\Delta/\Delta_0)^2 = 1 - (H/H_{c2})^2$ well, as shown in Fig. 2(c). H_{c2} for the nanoribbon (11 ML \times 60 nm) is 0.62 T, which is in good agreement with 0.63 T measured in Fig. 2(b). Since the ZBC depends on the quasiparticle lifetime used in the Dynes equation to fit the data, as well as energy gap Δ , these two methods should produce similar results.

Figure 3(a) displays the width dependence of H_{c2} , which is essentially linear in a range from 10 nm to 40 nm for all the thicknesses studied at $T=4.32$ K. An exception is the 13 ML \times 50 nm nanoribbon, the H_{c2} deviates greatly from the linear fit [indicated by the arrow in Fig. 3(a)]. It probably depicts a dimensional crossover from two dimensions to one dimension, as reported previously in Pb nanowires,^{10,11} consistent with the discussion of T_c described above.

From the H_{c2} and the general GL expression $\xi_{GL}(T) = \xi_{GL}(0)(1 - T/T_c)^{-1/2}$, as well as $\xi(4.3 \text{ K}) = [\Phi_0/2\pi H_{c2}(4.3 \text{ K})]^{1/2}$ [Φ_0 is the magnetic flux quantum (2.07×10^{-7} G cm²)], the GL coherence length $\xi_{GL}(0)$ can be deduced. The result for the nanoribbons of 13ML thickness is shown in Fig. 3(b). An overall reduction in $\xi_{GL}(0)$ is noted. The reduction in ξ_{GL} is primarily caused by the small electronic mean-free $l(w)$ length due to transverse surface scattering. Based on the GL “full-value” formula,²⁹

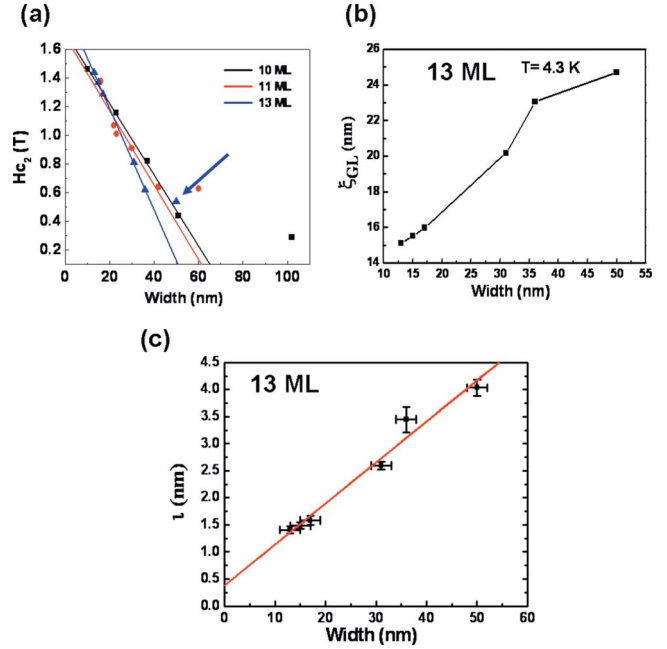


FIG. 3. (Color online) (a) Width dependence of the upper critical magnetic field (H_{c2}) of Pb nanoribbons with a thickness of 10, 11, and 13 ML ($T=4.32$ K). (b) Width dependence of the coherence length ξ of 13 ML nanoribbon. (c) Width dependence of the electronic mean-free path l of 13 ML Pb nanoribbon.

$$\xi(w, d) = 0.739[\xi_0'^{-2} + 0.747(\xi_0' l)^{-1}]^{-1/2},$$

one can obtain all $l(w, d)$ at 0 K with w and d being the width and thickness, respectively. Instead of ξ_0 , the normalized coherence length ξ_0' from $\xi_0' T_c^{\text{ribbon}} = \xi_0 T_c$ is used in the above expression to explain the lowering of T_c in the nanoribbons.³⁰ As shown in Fig. 3(c), $l(w, 3.7 \text{ nm})$ scales with w as $0.37 + 0.075w$. For example, the mean-free lengths are 1.3 and 3.1 nm for the 13 and 36 nm wide nanoribbons, respectively, with a thickness of 3.7 nm. They are significantly smaller than that of the 2D film at the same thickness (about 7.4 nm).³¹ A reduced mean-free length normally reduces coherence length and increases the magnetic field penetration length; hence vortices would not be expected in such narrow nanoribbons, and the linear dependent of ZBC on H does not exist.

In summary, by using temperature- and magnetic-field-dependent STM/STS, we have systematically investigated the superconductivity of single crystalline Pb nanoribbons with well-controlled dimensions and sizes. A dimensional crossover from two dimensions to one dimension is identified. Furthermore, the result reveals that robust superconductivity can persist even in crystalline Pb nanoribbons with a very small width (~ 10 nm) and thickness (~ 2.9 nm). We hope that our study can stimulate further experimental and theoretical interest toward understanding the superconducting behaviors in the 1D limit.

*Corresponding author; xcma@aphy.iphy.ac.cn

- ¹A. Bezryadin, C. N. Lau, and M. Tinkham, *Nature* (London) **404**, 971 (2000).
- ²K. Y. Arutyunov, D. S. Golubev, and A. D. Zaikin, *Phys. Rep.* **464**, 1 (2008).
- ³D. S. Golubev and A. D. Zaikin, *Phys. Rev. B* **64**, 014504 (2001).
- ⁴N. Giordano, *Phys. Rev. Lett.* **61**, 2137 (1988).
- ⁵J. Wang, C. Shi, M. Tian, Q. Zhang, N. Kumar, J. K. Jain, T. E. Mallouk, and M. H. W. Chan, *Phys. Rev. Lett.* **102**, 247003 (2009).
- ⁶J. Wang, X. C. Ma, L. Lu, A. Jin, C. Gu, X. C. Xie, J. Jia, X. Chen, and Q. Xue, *Appl. Phys. Lett.* **92**, 233119 (2008).
- ⁷M. L. Tian, J. G. Wang, J. S. Kurtz, Y. Liu, and M. H. W. Chan, *Phys. Rev. B* **71**, 104521 (2005).
- ⁸M. L. Tian, N. Kumar, S. Y. Xu, J. G. Guo, J. S. Kurtz, and M. H. W. Chan, *Phys. Rev. Lett.* **95**, 076802 (2005).
- ⁹J. Hua, Z. L. Xiao, A. Imre, S. H. Yu, U. Patel, L. E. Ocola, R. Divan, A. Koshelev, J. Pearson, U. Welp, and W. K. Kwok, *Phys. Rev. Lett.* **101**, 077003 (2008).
- ¹⁰F. Sharifi, A. V. Herzog, and R. C. Dynes, *Phys. Rev. Lett.* **71**, 428 (1993).
- ¹¹P. Xiong, A. V. Herzon, and R. C. Dynes, *Phys. Rev. Lett.* **78**, 927 (1997).
- ¹²R. A. Smith, B. S. Handy, and V. Ambegaokar, *Phys. Rev. B* **63**, 094513 (2001).
- ¹³M. Zgirski, K.-P. Riikonen, V. Touboltsev, and K. Arutyunov, *Nano Lett.* **5**, 1029 (2005).
- ¹⁴S. Michotte, L. Piraux, S. Dubois, F. Pailloux, G. Stenuit, and J. Govaerts, *Physica C* **377**, 267 (2002).
- ¹⁵S. Michotte, *Int. J. Mod. Phys. B* **17**, 4601 (2003).
- ¹⁶A. Rogachev, A. T. Bollinger, and A. Bezryadin, *Phys. Rev. Lett.* **94**, 017004 (2005).
- ¹⁷T. G. Sorop and L. J. Jongh, *Phys. Rev. B* **75**, 014510 (2007).
- ¹⁸U. Patel, S. Avci, Z. L. Xiao, J. Hua, S. H. Yu, Y. Ito, R. Divan, L. E. Ocola, C. Zheng, H. Claus, J. Hiller, U. Welp, D. J. Miller, and W. K. Kwok, *Appl. Phys. Lett.* **91**, 162508 (2007).
- ¹⁹Z. L. Guan, R. Wu, Y. X. Ning, C. L. Song, L. Tang, D. Hao, Xu-Cun Ma, J. F. Jia, X. Chen, Q. K. Xue, Z. M. Liao, and D. P. Yu, *Appl. Phys. Lett.* **93**, 023115 (2008).
- ²⁰Y. Guo, Y. F. Zhang, X. Y. Bao, T. Z. Han, Z. Tang, L. X. Zhang, W. G. Zhu, E. G. Wang, Q. Niu, Z. Q. Qiu, J. F. Jia, Z. X. Zhao, and Q. K. Xue, *Science* **306**, 1915 (2004).
- ²¹D. Eom, S. Qin, M. Y. Chou, and C. K. Shih, *Phys. Rev. Lett.* **96**, 027005 (2006).
- ²²T. Nishio, M. Ono, T. Eguchi, H. Sakata, and Y. Hasegawa, *Appl. Phys. Lett.* **88**, 113115 (2006).
- ²³T. Nishio, T. An, A. Nomura, K. Miyachi, T. Eguchi, H. Sakata, S. Lin, N. Hayashi, N. Nakai, M. Machida, and Y. Hasegawa, *Phys. Rev. Lett.* **101**, 167001 (2008).
- ²⁴Y. X. Ning, C. L. Song, Z. L. Guan, X. C. Ma, X. Chen, J. F. Jia, and Q. K. Xue, *EPL* **85**, 27004 (2009).
- ²⁵S. Qin, J. Kim, Q. Niu, and C. K. Shih, *Science* **324**, 1314 (2009).
- ²⁶C. Brun, I-Po Hong, François Patthey, I. Yu. Sklyadneva, R. Heid, P. M. Echenique, K. P. Bohnen, E. V. Chulkov, and Wolf-Dieter Schneider, *Phys. Rev. Lett.* **102**, 207002 (2009).
- ²⁷D. H. Douglass, *Phys. Rev. Lett.* **7**, 14 (1961).
- ²⁸R. C. Dynes, V. Narayanamurti, and J. P. Garno, *Phys. Rev. Lett.* **41**, 1509 (1978).
- ²⁹M. Tinkham, *Introduction to Superconductivity*, 2nd ed. (McGraw-Hill, New York, 1996).
- ³⁰T. P. Orlando, E. J. McNiff, Jr., S. Foner, and M. R. Beasley, *Phys. Rev. B* **19**, 4545 (1979).
- ³¹M. M. Özer, J. R. Thompson, and H. H. Weitering, *Nat. Phys.* **2**, 173 (2006).